ISSN 1070-4272, Russian Journal of Applied Chemistry, 2009, Vol. 82, No. 2, pp. 307−311. © Pleiades Publishing, Ltd., 2009.
Original Russian Text © S.S. Sigaeva, P.G. Tsyrul'nikov, D.A. Shlyapin, T.S. Dorofeeva, N.N. Voitenko, V.I. Vershinin, N.A. Davletkil'deev, G.B. Kuznetsov, S.L. Kanashenko, 2009, published in Zhurnal Prikladnoi Khimii, 2009, Vol. 82, No. 2, pp. 313−316.

ORGANIC SYNTHESIS AND INDUSTRIAL ORGANIC CHEMISTRY

Catalysts of Methane Pyrolysis: Pretreatment and Study of Fechral Support

S. S. Sigaeva, P. G. Tsyrul'nikov, D. A. Shlyapin, T. S. Dorofeeva, N. N. Voitenko, V. I. Vershinin, N. A. Davletkil'deev, G. B. Kuznetsov, and S. L. Kanashenko

Institute of Hydrocarbon Processing Problems, Siberian Branch, Russian Academy of Sciences, Omsk, Russia
Dostoevsky State University, Omsk, Russia
Hitachi High-Technologies, Moscow, Russia

Received April 9, 2008

Abstract—The pretreatment of Fechral support for preparing a methane pyrolysis catalyst was studied. The Fechral support after high-temperature (1000°C) treatment in air was examined by atomic force microscopy, scanning electron microscopy with chemical analysis, and X-ray phase analysis of the surface layer. The morphological, chemical, and phase changes on the support surface were studied. A mechanism of formation of the dispersed α-Al_2O_3 phase on the Fechral surface was suggested.

DOI: 10.1134/S1070427209020268

Efficient utilization of hydrocarbon resources and development of new resource-saving and environmentally clean technologies acquire growing importance today. From the environmental viewpoint, methane is the cleanest natural energy source. Methane is used today in industry for production of energy and also of synthesis gas, hydrogen, halogen derivatives, and HCN [1]. Markedly growing interest in the hydrogen fuel and its use in means of transportation [2–4] makes problems of hydrogen production and storage urgent. It is suggested to use hydrogen for direct combustion in internal combustion engines, as additives to organic fuel, but mainly in fuel cells. Electric cars with fuel cells can be considerably more efficient than cars with internal combustion engines. Furthermore, the environmental advantages or fuel cells are obvious: only water vapor is formed in combustion of hydrogen.

Pure hydrogen can be prepared, in particular, by endothermic decomposition of methane (main component of natural gas) on an appropriate catalysts, e.g., on palladium alloys [5]. The most active in this process are catalysts based on transition metals, primarily Ni, Co, and Fe applied onto Al_2O_3- or SiO_2-based supports [6–8]. The generally accepted mechanism of methane decomposition, carbide cycle mechanism [7–12], suggests initial decomposition of methane on less closely packed faces (100, 010) of metal crystals, dissolution of carbon in the crystal up to saturation, and formation of graphite layers on the close-packed (111) face. The propagating carbon thread can detach the crystal from the support and transfer it into the intergrain space. In the course of the subsequent oxidative regeneration of the catalyst, dispersed particles of the metal (or oxide formed) are removed with the gas flow. In the process, the catalyst is destroyed.

Presumably, the use of heat-resistant all-metal supports with a strong surface oxide layer containing active elements would allow preparation of new catalysts of methane decomposition, which not only would be interesting for basic science but also would withstand repeated regenerations. In this study we took as support Fechral, an alloy used, in particular, in production of metallic blocks for automobile exhaust afterburning.

The surface of the initial Fechral alloy has almost no adsorption centers. This complicates application of nickel and other iron-group metals onto the support surface. The use of Fechral as support requires increasing its specific surface area, forming appropriate morphology, and changing the composition of the surface layer, which can be attained by pretreatment.

The goal of this study was to develop a procedure and find conditions of Fechral treatment for developing its

surface, and also to study the morphology of the Fechral surface and phase transformations occurring on it.

EXPERIMENTAL

The starting material was a wire of Cr23Al5Ti Fechral alloy, 0.25 mm in diameter, produced by Elektrostal' Metallurgical Plant, Joint-Stock Company. According to GOST (State Standard) 12766 1–90, this iron-based alloy contains (wt %) Cr 22-24, Al 5–58, and also impurities of Ni up to 0.6, Ti and Si up to 0.5, Mn up to 0.3, Ca and Ce up to 0.1, C up to 0.05, and S up to 0.015.

The wire was cut in pieces 0.3–1 cm long, degreased by washing in acetone, and calcined in air in a muffle furnace at 1000°C (preliminary experiments showed that this treatment temperature ensures the optimal extent of changes in the surface layer, combined with sufficient strength). The calcination time was varied from 2 to 21 h, and the samples were weighed before and after calcination. Then 10–15 g of the calcined support in a quartz reactor was placed in a tubular muffle furnace and reduced at 700°C in a hydrogen flow for 2 h before testing in methane pyrolysis.

To study the phase transformations occurring in the course of heat treatment of the support, the surface layer of the calcined and initial samples was separated mechanically, and its phase composition was studied by powder X-ray diffraction with a DRON-3 diffractometer using $Cu_{K\alpha}$ radiation.

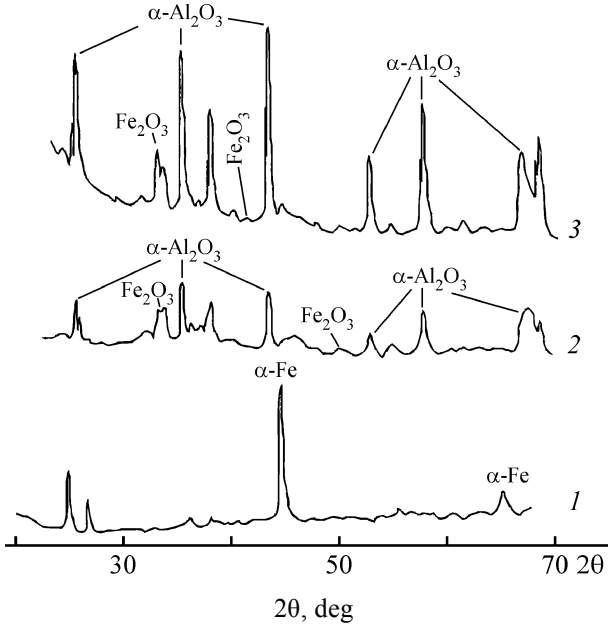

Fig. 1. X-ray diffraction patterns of the (*1*) initial support and that calcined in air at 1000°C for (*2*) 12 and (*3*) 21 h. (2θ) Bragg angle.

The initial support and the ready catalyst were examined by atomic force microscopy (AFM). For this purpose, Fechral wire was compacted in pellets 10 mm in diameter and 0.5–1 mm thick under a pressure of 160 atm in a mold. The pellets were polished with emery paper and with chromium sesquioxide paste, degreased, and subjected to the same treatment as the wire samples, i.e, were calcined in air at 1000°C and reduced in a hydrogen flow at 700°C. Then the samples were subjected to microscopic examination with a Solver PRO scanning electron microscope using an NSG01 probe sensor. The same samples were studied by scanning electron microscopy. In so doing, we used an S3400N electron microscope with a Hitachi High-Technologies attachment for chemical analysis.

Only iron is identified in the initial wire by X-ray phase analysis (XPA) (Fig. 1). Chromium is not detected because its peaks are obscured by iron peaks, and the aluminum content of Fechral (~5%) is insufficient for its detection by low-sensitive XPA method.

After calcination, peaks of oxidized forms of aluminum and iron appear in the diffraction patterns. These peaks belong to α-Al_2O_3 (corundum) and Fe_2O_3 (hematite), with the corundum peaks being considerably more intense. With increasing calcination time, the relative intensity of corundum peaks increases, and that of hematite peaks decreases. Hence, the experimentally observed weight gain of the samples after calcination can be interpreted as follows: Under the action of high temperature, aluminum whose melting point is 660°C diffuses to the surface and is oxidized there with atmospheric oxygen, transforming into α-Al_2O_3. Simultaneous oxidation of iron can be neglected, the more so as hematite is then partially reduced in a hydrogen stream, whereas corundum is not reduced.

It is known [13] that calcination of a foamed material based on Fechral at 500–1000°C leads to appearance of the α-Al_2O_3 phase in the surface layer owing to diffusion of aluminum atoms to the sample surface and their subsequent oxidation. At 500°C, aluminum oxide crystals exist in a small amount, but at 900°C the sample surface is fully coated with them. Further increase in the temperature affects the morphology of the crystals: They agglomerate to form spheroidal particles. In the process, the thickness of the oxide layer increases.

Calcination of the Fechral wire should also be accompanied by these processes. However, the wire

is more resistant than foamed Fechral to oxidation with atmospheric oxygen. Therefore, on the basis of preliminary experiments we chose a higher calcination temperature (1000°C).

In the examined interval of calcination times, the relative change in the support weight is minor (about 1%). The weight gain is well reproduced, and the weight linearly grows with time (Fig. 2). This fact indicates that the rate of aluminum diffusion from the bulk of the alloy to the sample surface is approximately constant. Assuming that the weight gain is exclusively due to formation of corundum from aluminum diffusing to the sample surface, we calculated that approximately 40% of aluminum present in the initial sample diffused to the sample surface during calcination (21 h) and was oxidized there. Apparently, in the course of further calcination the aluminum diffusion will decelerate because of smaller concentration gradient between the bulk and surface of the sample.

To understand how Fechral calcination affects the surface layer morphology, we examined the samples by AFM. Visually the initial support surface looks like a common polished metal surface. The maximal roughness height according to AFM data is 0.18 μm. After calcination at 1000°C and reduction in a hydrogen flow, the surface morphology changes essentially (Fig. 3). A new phase, α-Al_2O_3, appears in the form of nodules covering virtually the whole surface. The maximal height drop is 1 μm. It should be noted that a similar pattern was obtained previously [14] with a scanning electron microscope. The material examined in [14] was similar (Fe–Cr–Al alloy, 75 : 20 : 5), but the surface activation procedure was not reported.

From the AFM data we calculated the roughness R of the samples. By the roughness we understand here the mean height of the α-Al_2O_3 particles formed. The dependence of the roughness on the calcination time passes through an extremum (Fig. 4).

The roughness appeared to be maximal in samples calcined for 8 h and then reduced. Longer calcination (12 h) leads to a decrease in the mean height of the aluminum oxide particles formed. This may be due to filling of the space between the initial particles (nodules) of corundum due to the continuing oxidation of aluminum diffusing from the bulk and reduction of iron oxide with hydrogen. As a result, the detectable part of surface formations becomes smaller.

Further study of the morphology and chemical composition of the Fechral wire surface before and after calcination was performed by scanning electron microscopy. Figure 5a shows the initial Fechral surface. The elemental composition of the surface is approximately equal in different points and corresponds to the bulk composition of Fechral declared by the producer. The observed macrodefects of the surface appear apparently in step of wire drawing through dies.

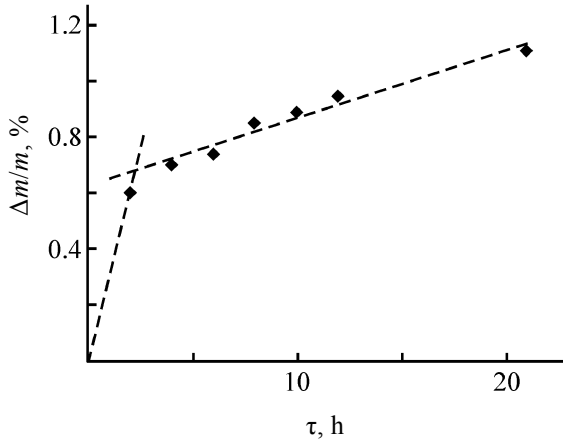

Fig. 2. Relative change in the support surface $\Delta m/m$ as a function of calcination time τ.

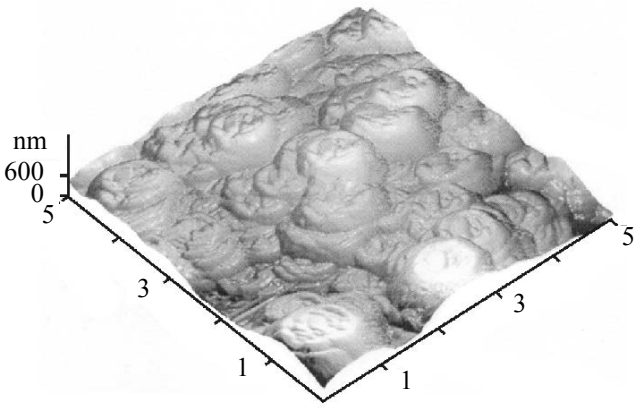

Fig. 3. AFM image of the pelletized support (160 atm) after calcination at 1000°C for 12 h and reduction in a hydrogen flow at 700°C (15 × 15 μm).

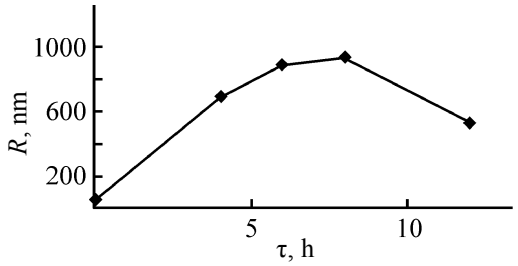

Fig. 4. Roughness R of the support surface as a function of calcination time τ (AFM data).

(a)

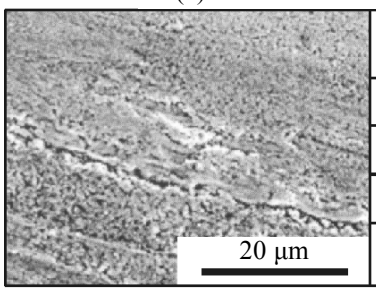

Element	c
Fe	66.32
Cr	21.56
Al	5.84
O	5.73

(b)

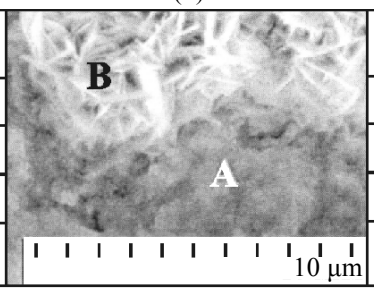

Element	c	
	A	B
Fe	47.39	4.90
Cr	12.06	1.46
Al	11.82	44.06
O	28.67	49.62

Fig. 5. SEM images (with EDAX analysis data) of the surface of the (a) initial support and (b) that calcined for 21 h at 1000°C.

After the high-temperature treatment, the Fechral surface becomes very nonuniform in morphology and uneven (Fig. 5). Morphologically different areas (A and B) differ also in the chemical composition. Areas of type A contain considerably more aluminum and oxygen than the initial surface of untreated Fechral, which is consistent with the XPA data on the formation of α-Al_2O_3 on the surface. Areas of type B are characterized by the needle-like structure. Rosettes on the surface of the calcined support (areas B) contain still more aluminum and oxygen than areas A, and the amount of Fe and Cr in these areas is, on the contrary, very low. The elemental composition of the solid phase in areas B approaches that of pure corundum.

The surface nonuniformity observed by scanning electron microscopy suggests that the directional migration of aluminum atoms to the surface occurs more actively along intercrystallite boundaries of the Fechral alloy. The oxide layer formed in the course of oxidative treatment is very strong. It is not broken even after oxidative treatment of the sample at 1100°C for 20 h.

It should be noted that examination by AFM (method providing higher resolution) revealed no coarse formations (rosettes). This difference for the two methods can be attributed to different procedures of support pretreatment. For AFM examination, samples before heat treatment were pelletized under a pressure of 160 atm, heat-treated, and reduced with hydrogen. Presumably, compaction made intercrystallite boundaries narrower (healing), which hindered the surface oxidation in the course of the heat treatment. Only nodules approximately 1 μm in size can be seen in the AFM image of such sample (Fig. 1). The surface of the initial wire was oxidized more readily and to a greater extent compared to the pellet, which led to formation of coarser rosettes (~7 μm) observed by scanning electron microscopy.

CONCLUSION

As a result of phase transitions that accompany the heat treatment, with radical changes in the morphology of the Fechral surface, the roughness and geometric surface area of the support become several times higher, which favors stronger fixation of the active component on the surface of the Fechral support.

ACKNOWLEDGMENTS

The authors are grateful to K.A. Kulakovskii and Cand. Sci. (Chem.) A.V. Kuznetsov ("Yurpromkonsalting," Moscow) for the support of the study and submission of the materials for the experiments.

REFERENCES

1. Arutyunov, V.S. and Krylov, O.V., *Okislitel'nye prevrashcheniya metana* (Oxidative Transformations of Methane), Moscow: Nauka, 1998.
2. Hellmont, R. and von Eberle, U., *J. Power Sources*, 2007, vol. 165, pp. 833–843.
3. Halk, S.G. and Miller, J.F., *J. Power Sources*, 2006, vol. 159, pp. 73–80.
4. Satyapal, S., Petrovic, J., Read, C., et al., *Catal. Today*, 2007, vol. 120, pp. 246–256.
5. Ogihara, H., Takenaka, S., Yamanaka, I., et al. , *J. Catal.*, 2006, vol. 238, pp. 353–360.
6. Li, Y., Zhang, B., Xie, X., et al., *J. Catal.*, 2006, vol. 238, pp. 412–424.
7. Fenelonov, B.V., *Vvedenie v fizicheskuyu khimiyu formirovaniya supramolekulyarnoi struktury adsorbentov i katalizatorov* (Introduction to Physical Chemistry of Formation of Supramolecular Structure of Adsorbents and Catalysts), Novosibirsk: Sib. Otd. Ross. Akad. Nauk, 2004.

8. Chesnokov, V.V., Zaikovskii, V.I., Buyanov, R.A., et al., *Catal. Today*, 1995, vol. 24, p. 265.
9. Zaikovskii, V.I., Chesnokov, V.V., and Byanov, R.A., Appl. Catal., 1988, vol. 38, pp. 41–52.
10. Chesnokov, V.V., Zaikovskii, V.I., Buyanov, R.A., et al., *Kinet. Katal.*, 1994, vol. 35, pp. 146–151.
11. Buyanov, R.A. and Chesnokov, V.V., *Khim. Inter. Ustoich. Razv*., 1995, vol. 3, pp. 177–186.
12. Buyanov, R.A. and Chesnokov, V.V., *Katal. Prom–sti.,* 2006, no. 6, pp. 3–15.
13. Giani, L., Cristiani, C., Groppi, G., and Tronconi, E., *Appl. Catal. B: Environmental*, 2006, vol. 62, p. 121.
14. Menon, P.G., Zwinkels, M.F.M., Johansson, E.M., and Järäs, S.G., *Kinet. Katal*., 1998, vol. 39, p. 670.